UNIVERSITÀ DEGLI STUDI DI PADOVA

SCUOLA DI SCIENZE
Dipartimento di Geoscienze
Direttore Prof. Nicola Surian

TESI DI LAUREA MAGISTRALE IN GEOLOGIA AMBIENTALE E DINAMICA DELLA TERRA

Microplastic trapping in sediments during tractional deposition an experimental approach

Relatore: Prof. Massimiliano Zattin
Correlatore: Prof. Massimiliano Ghinassi
Dr. Francesca Uguagliati

Laureanda: Melissa Kozhaya
Matricola: 2072043

ANNO ACCADEMICO 2023-2024

To my father, mother and aunt, who accompanied me on this journey with support and love,
To my sister and my brothers, my nieces and my nephew,
To all the people in my village in Lebanon, friends, neighbors,
To my priest, spiritual guide who listened to me with patience, love, and enriched my soul with Faith and Hope,
To my dear friends I met on the path, with whom I felt home, and who lead me to develop myself further, Mahla Moradi, Omneya Ahmad, Nahed Ahmad, Judy Eter, Christelle Maaiki, Mohamad Ebid,
To every person who decided to work on self,
I dedicate this thesis.
Likewise, I dedicate this work to my Lord - Jesus Christ and St. Anthony of Padova, with whom I felt protected, loved, and blessed.

Content

Abstract

Microplastics (MPs) are a growing environmental concern due to their prevalence in aquatic ecosystems and the potential risks they pose to biodiversity. This study focuses on the behavior and distribution of polyamide (PA) and polyester (PES) fibers in a controlled experimental flume simulating sediment transport dynamics found in riverine systems. Using a combination of controlled MP inputs and reduced concentration analyses, the research aims to explore the differences in fiber behavior, particularly in terms of their concentration in water columns and sediment layers. The findings reveal that PES fibers, despite their higher density, remain suspended in the water column for longer periods due to hydrodynamic conditions and fiber size. The study underscores the importance of considering attributes like fiber surface area and length, rather than relying solely on mass-based metrics, for a comprehensive understanding of MP behavior in aquatic environments.

Riassunto

Le microplastiche (MPs) rappresentano una crescente preoccupazione ambientale a causa della loro diffusione negli ecosistemi acquatici e dei potenziali rischi che pongono per la biodiversità. Questo studio si concentra sul comportamento e sulla distribuzione delle fibre di poliammide (PA) e poliestere (PES) in un flume sperimentale controllato che simula le dinamiche di trasporto dei sedimenti nei sistemi fluviali. Utilizzando una combinazione di input controllati di MPs e analisi a concentrazione ridotta, la ricerca mira a esplorare le differenze nel comportamento delle fibre, in particolare in termini di concentrazione nella colonna d'acqua e negli strati di sedimenti. I risultati rivelano che le fibre di PES, nonostante la loro maggiore densità, rimangono sospese nella colonna d'acqua per periodi più lunghi a causa delle condizioni idrodinamiche e delle dimensioni delle fibre. Lo studio sottolinea l'importanza di considerare attributi come la superficie e la lunghezza delle fibre, piuttosto che basarsi esclusivamente su parametri legati alla massa, per comprendere meglio il comportamento delle MPs negli ambienti acquatici.

1. Introduction

Plastic is a synthetic polymer ubiquitous in everyday products due to its durable and persistent nature, making it suitable for numerous applications (PlascticEurope, 2021). According to a 2023 report by the Geneva Environment Network, the production and consequent waste of plastic worldwide have increased exponentially since 1950. This continuous growth has led to the widespread dispersion and accumulation of plastics in the environment, causing significant contamination across the Earth's surface (Barnes et al., 2009).

Plastics come in various shapes and sizes, with those smaller than 5 mm being classified as MPs. Primary MPs are intentionally manufactured to be small and include nurdles, glitter, and microbeads found in cosmetics and personal care products. In contrast, secondary MPs arise from the degradation of larger plastic items, which can occur through mechanical degradation, chemical exposure, UV radiation, or biological processes (Hernandez et al., 2017; Horton et al., 2017; Napper & Thompson, 2016; Rillig, 2012). Additionally, synthetic textiles, including PES, nylon, and acrylic, contribute significantly to secondary MPs, as individual fibers are released during washing and enter wastewater systems (De Falco et al., 2018). Each laundry cycle can release up to 1,900 fibers per garment (Browne et al., 2011) or around 0.1 mg of fibers per gram of fabric, resulting in a loss of roughly 0.01% of the material washed (Hernandez et al., 2017).

The environmental impact of MPs is significant, as they pose potential toxicity risks, durability, and persistence (Hidalgo-Ruz et al., 2012; Lusher et al., 2014). MPs can also serve as vectors of contaminants, further amplifying their ecological threat (Avio et al., 2015; Browne et al., 2013; Chua et al., 2014).

With an estimated annual riverine flux of up to 2.41 million tons, rivers are critical pathways for transporting MPs into the ocean (Lebreton et al., 2017). In particular, the dynamics of MP transport in rivers are influenced by both horizontal and vertical distribution processes. Horizontal distribution is driven by water flow velocity, precipitation, and wind currents, determining the movement of debris into water bodies. In contrast, vertical distribution involves processes like turbulent mixing, biota transfer, and biological fouling, affecting the deposition and resuspension of MPs (Xia et al., 2020; Liu et al., 2022; Coyle et al., 2020; Welden & Lusher, 2017; Kooi et al., 2017) . Additionally, rivers can act as temporary reservoirs for these pollutants (Besseling et al., 2017). River sediments serve as microenvironments for various microflora and fauna, playing vital roles in biogeochemical cycling (Lu et al., 2022). However, recent studies indicate that sediments can also accumulate heavy metals, toxic pollutants, pathogens, and MPs, highlighting their role in assessing environmental contamination (Vimalkumar et al., 2018; Tamilmani & Venkatesan, 2021; Sun et al., 2022; Toraskar et al., 2022).

The density of MP particles varies widely, ranging from less than 0.01 g/cm^3 for expanded polystyrene foam to 2.1–2.3 g/cm^3 for polytetrafluoroethylene (Teflon) (Chubarenko et al., 2018). Lighter MPs generally remain suspended in the water column but can sink over time as biofilm accumulates on their surfaces or through interactions with suspended clay particles, which increase their overall density (Nel et al., 2017; Waldschläger et al., 2020; Kaiser et al., 2017). In contrast, denser MPs tend to sink immediately upon entering the environment and are often found in sediments and fish samples (Zhang et al., 2020). Increased flow velocities can remobilize these particles along with sediment, making river sediments both sinks and sources of MP pollutants (Ballent et al., 2016; Nel et al., 2017; Liro et al., 2020). When investigating the transport of MPs in river systems, it's essential to account for the influence of fine cohesive sediments present in the environment. These sediments can attach to MPs, creating denser aggregates that are capable of being transported as separate particles within the bedload (Corcoran et al., 2020; Chubarenko et al., 2016; Sekudewicz et al., 2021). The movement behavior of MPs bound to sediments, which differs from that of floating debris, is still under explored. This is especially true when considering the various types of MPs and how they interact with different river sediments, which may or may not lead to the formation of aggregates (Waldschläger & Schüttrumpf, 2019b; Yang et al., 2021).

Several studies indicate that the transport mechanisms of MPs and sediments in rivers exhibit similarities since they follow the same hydrodynamic principles (Enders et al., 2019; Cowger et al., 2021; Waldschläger & Schüttrumpf, 2019a; Francalanci et al., 2021). However, it is essential to note that MPs display diversity in terms of density, particle size, and shape while natural sediments are commonly generalized as spherical and uniformly size-distributed (Waldschläger et al., 2022).

This study aims to investigate and quantify the mobility of MPs under controlled unidirectional traction flow conditions. An experimental flume, specifically designed to replicate natural sediment transport dynamics, is employed, utilizing a controlled mixture of sediments and water. This research investigates the mobility and interactions of MPs, addressing a current gap in understanding how two different types of MPs are transported and accumulate in river sediments. Additionally, the study compares the MPs carried by the water flow with those that become embedded and retained within the sediment matrix.

2. Methodology

Research facility

The experimental flume utilized in this study is a fixed-bank channel apparatus with 0º inclination. It measures 4 meters in length, 30 centimeters in width, and 50 cm in depth (figure 1), allowing precise control over experimental variables such as flow velocity, sediment grain size, and water depth. Water circulates through the flume using a system connected to two tanks, each measuring 110 cm by 90 cm with a height of 66 cm (figure 1/a-b). These tanks are typically filled to a level of approximately 50 cm, providing a water volume of about 495 l per tank. This arrangement ensures a sufficient water supply for continuous flow throughout the experiments, with a total capacity of approximately 990 l from both tanks combined.

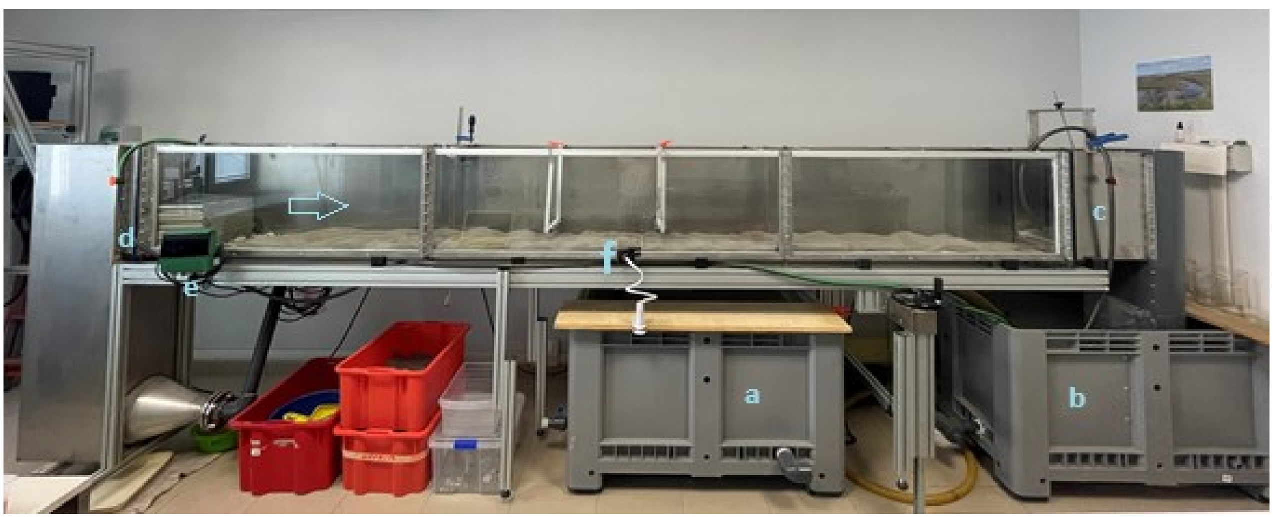

Figure 1: Flume setup. The blue arrow shows the water flow direction. "a-b" are the two tanks. "c-d" are the pipes with valves connected to the small pump. "e" is the flow meter. "f" is the GoPro HERO 9 camera

To manage water flow, the system is equipped with two pumps. The primary pump (figure 2), used during the initial filling phase and the experiment, has a discharge rate of 9 liters per second (33.5 cubic meters per hour), ensuring a rapid and consistent water supply. Additionally, a smaller pump is employed (figure 3) connected to two pipes equipped with valves (figure 1/c-d), which regulate the water flow precisely, thereby maintaining the experimental conditions without affecting the bedform.

Figure 2: The primary pump

Figure 3: The small pump

Figure 4: The bypass system

The flume also features a bypass system (figure 4), which plays a crucial role in managing flow during pump operation. When the primary pump is activated, the bypass is open to divert excess water, allowing for a gradual increase in flow and preventing sudden pressure spikes that could destabilize the experimental conditions. Flow is monitored and controlled using a flowmeter (figure 1/e).

At the upstream end of the flume, a pipe barrier is installed to break and evenly distribute the incoming water (figure 5), preventing localized erosion and ensuring a uniform flow across the channel width. Moreover, directly downstream of this pipe barrier, a layer of gravel (figure 5) is placed to further stabilize the flow and reduce turbulence, which is essential for maintaining a consistent sediment bed.

Figure 5: Pipes barrier with gravels downstream the barrier

Figure 6: 3D sandy ripple form

A downstream barrier is used to regulate the water depth within the flume, adjustable to alter the water level and simulate different hydraulic conditions. Additionally, barriers are strategically placed upstream and downstream of the flume to gradually decrease the water level as needed, providing flexibility in the experimental setup. This configuration allowed for the development of 3D sandy ripple forms in the flume, with water depth set to 11 cm, and the ripples, measuring approximately 2-3 cm in height, migrating at a rate of 0.7 cm/min (figure 6).

In addition, a GoPro HERO 9 camera (figure 1/f) was used to record the experiments in time-lapse mode. The camera was positioned on the side of the flume to capture the movement of the sediment bed. It was set to linear lens mode to reduce distortion and ensure an accurate representation of the bed dynamics. Video format was selected to allow continuous recording, and the interval was set to 'no limit,' enabling uninterrupted capture of the experiments.

Sediment

The flume bed was composed of a mixture of fine, medium, and coarse sand, with grain sizes ranging from approximately 0.125 mm to 2 mm and density of 2.65 g/cm^3. The sand was evenly distributed along the entire length of the flume, forming a uniform bed with a thickness of approximately 3 cm.

Microplastics

Two types of MPs particles were used: i) 500 µm long green PA fibers, with a density of 1.14 g/cm³ and a diameter of 19 µm, ii) 500 µm long black PES fibers with a density of 1.38 g/cm³ and diameters ranging from 16.6 to 19.7 µm (figure 7). These MP particles were kept in continuous motion within the water flow.

Figure 7: 300 mg of MPs in 2 transparent boxes. PA fibers (in the middle). PES fibers (on the right)

With the flume setup established and the sediment bed prepared, the study involved two main experiments, with two runs conducted for each.

a. Experiment 1: Controlled MPs input

In Experiment 1, we introduced 300 mg each of PA and PES into the fixed-bank channel. The decision to use 300 mg for both materials was informed by relevant literature, ensuring consistency with similar studies (e.g. Ghinassi et al., 2023). To estimate the required fiber quantities, we first measured several different masses of fibers, placing them in small paper boats. Each boat was weighed using a Mettler Toledo XPR36 balance, and photographs of the boats were taken with a SONY ILCE-7RM3 camera set to 200 ISO, 300 dpi resolution (both vertical and horizontal), and no flash. The fibers were then counted manually using Photoshop's counting tool (table 1). After determining the mass, we calculated the required fiber concentrations based on the dimensions and total volume of the tanks. With each tank measuring 110 cm by 90 cm by 50 cm, the combined volume was approximately 1000 liters. This led to the introduction of 300 mg of PA, yielding a concentration of 15 fibers per liter, and 300 mg of PES, resulting in 40 fibers per liter.

	Green (g) and Black (b) Fibers						
Paper label	**Mass 1 (mg)**	**Mass 2 (mg)**	**Mass 3 (mg)**	**Average (mg)**	**Number of fibers**	**Mass of 1 fiber (mg)**	**Mass of 1 fiber (µg)**
1g	0.011	0.009	0.01	0.01	24	0.000416667	0.416667
2g	0.035	0.04	0.037	0.037333	101	0.000369637	0.369637
3g	0.02	0.024	0.022	0.022	189	0.000116402	0.116402
4g	0.037	0.044	0.047	0.042667	128	0.000333333	0.333333
5g	0.025	0.024	0.02	0.023	221	0.000104072	0.104072
6g	0.005	0.007	0.01	0.00733	66	0.000111111	0.111111
7g	0.063	0.065	0.064	0.064	307	0.000208469	0.208469
8g	0.033	0.032	0.032	0.03233	259	0.000124839	0.124839
9g	0.055	0.057	0.058	0.056667	228	0.000248538	0.248538
1b	0.008	0.01	0.012	0.01	169	$5.91716*10^{-5}$	0.059172
2b	0.026	0.028	0.03	0.028	254	0.000110236	0.110236
3b	0.027	0.03	0.03	0.029	349	$8.30946*10^{-5}$	0.083095
4b	0.027	0.028	0.029	0.028	305	$9.18033*10^{-5}$	0.91803
5b	0.012	0.013	0.016	0.013667	374	$3.65419*10^{-5}$	0.036542
6b	0.014	0.019	0.02	0.017667	201	$8.78939*10^{-5}$	0.087894
7b	0.005	0.002	0.006	0.004333	126	$3.43915*10^{-5}$	0.034392
8b	0.01	0.014	0.013	0.012333	136	$9.06863*10^{-5}$	0.090686
9b	0.003	0.006	0.007	0.005333	86	$6.210155*10^{-5}$	0.062016

Table 1: *Measurement data for PA and PES fibers*

b. Experiment 2: Flume run after MPs removal

Experiment 2 used the same fixed-bank channel setup and sediment conditions as Experiment 1 but was conducted with clean water, without the deliberate addition of any new MP fibers. However, because the sediment from Experiment 1 was not replaced, residual microplastics were still present in the system. This experiment was designed to simulate a scenario with a reduced concentration of microplastics, acknowledging that the removal process could not entirely clean the system. The goal was to observe how the remaining, lower concentration of microplastics behaved and how their distribution in the sediment and water column differed from Experiment 1, where a higher concentration of MPs was intentionally introduced. This approach allows for a comparison between the effects of high and reduced concentrations of microplastics within the same sediment environment.

Experimental procedure

The flume experimentation began with activating the pump while keeping the bypass valve open to start the water flow. Gradually, the bypass valve is closed to direct the water fully into the flume. As the flow establishes, the initial movement of sediment particles is observed. The system is then allowed to run for 2 hours, during which bedforms, such as ripples, propagate along the flume, achieving equilibrium.

Upon reaching equilibrium, the flow is stopped, and the drainage process is initiated. This involves opening the bypass valve, positioning two 5 cm gates (figure 8) at both the front and rear of the flume, and turning off the pump to allow the water to drain slowly over 2 hours without disturbing the sediment. Once the drainage is complete, 40 to 60 photos of the bed surface are captured using a NIKON CORPORATION camera with an ISO of 400, no flash, and a resolution of 300 dpi both horizontally and vertically. These photos are then used to create a 3D model of the bed by generating a dense point cloud.

Figure 8: 2 gates of 5 cm each

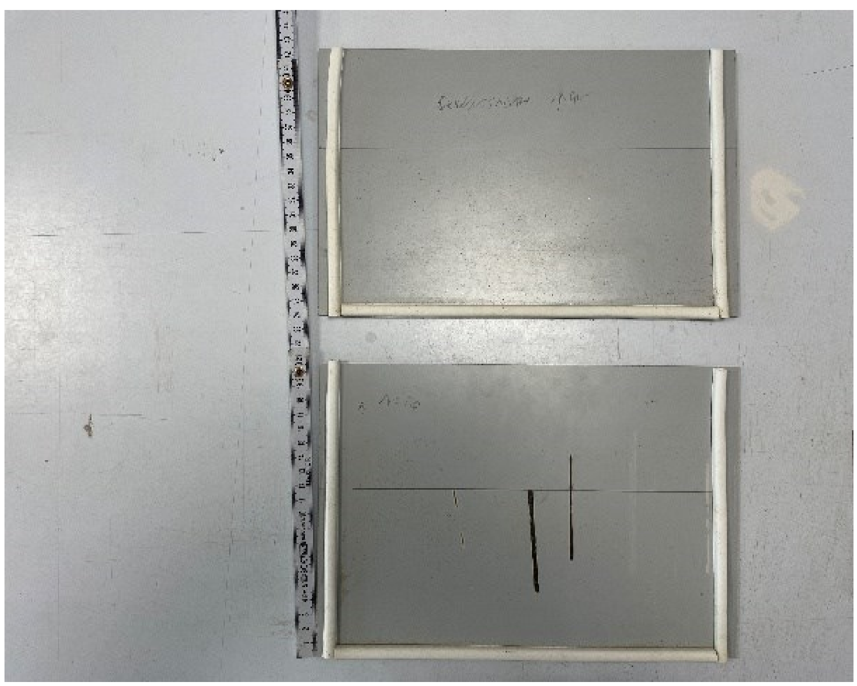

Figure 9: 2 high gates

Following this, the flume is gradually refilled using the small pump and high gates (figure 9) to prevent sediment disturbance. Once the water level reaches the desired height, the primary pump is restarted with the bypass open, and the gates are removed. While the water flows without disturbing the bed, fine red sand is introduced to mark the bedforms' position at the beginning of the experiment. It is important to note that the sediment transport conditions were identical to the first stage of transport after adding the marker. Thus, with the bypass valve closed, normal flow conditions are resumed, and the original flow velocity settings are reestablished.

During the subsequent 5-minute experimental run, water is continuously sampled from both the upper and the lower (close to the bed surface) part of the water column to monitor microplastic concentration during the whole experiment. Samples of 1600 ml of water were collected for experiments 1 and 2, while 1900 ml of water were collected for experiments 3 and 4, (figure 10). As sediment transport continues, the movement of the red sand markers is observed to assess sediment accumulation. After the experiment, the flow is terminated again, and the flume is drained using the same procedure as before.

Figure 10: Pipes for water samples from the upper part on the left and the lower part of the water column near the bed surface on the right

Finally, a second dense cloud of the bed surface is created after drainage to facilitate a DEM of Difference (DoD) analysis compared to the initial cloud, using the same procedure as before. Once the flume is dry and all the water has been drained, five sediment samples of approximately 20 g each are collected from above the marker (Figure 11). These samples are carefully gathered using a steel knife (Figure 12), wrapped in aluminum foil, and then transported to the laboratory for microplastic extraction and quantification.

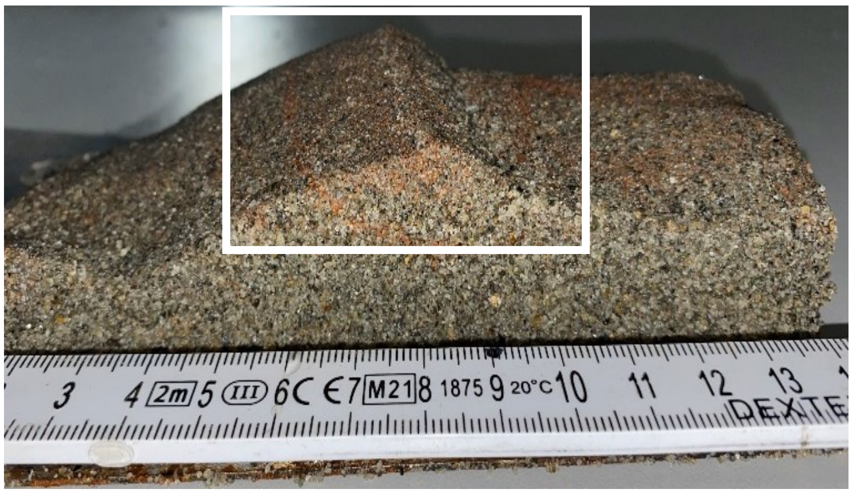

Figure 11: Sediment sampling site (white rectangle)

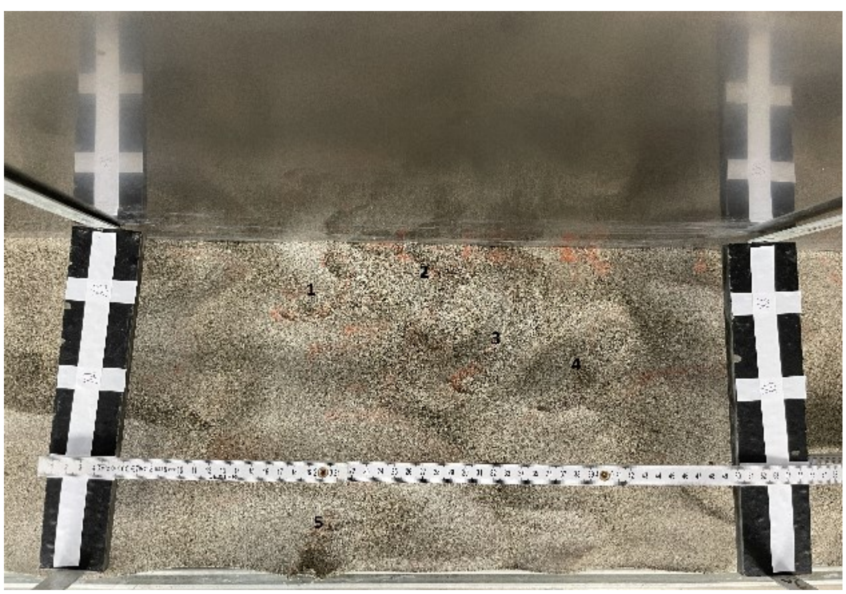

Figure 12: Real sampling from the flume (5 ripple sites)

Sediment and water sample analysis

For the water samples, each sample was filtered using a standard filtration apparatus. The filtration apparatus consists of a filter flask, a filter funnel, filter paper, and a vacuum pump. The filter flask is attached to the vacuum pump, and the filter funnel is placed on top of the flask. The total volume was divided into three portions to facilitate easier filtration and prevent the filters from clogging.

Sediment samples were dried at 40 degrees in the oven. Once dried, sediments were weighed and decanted in a 1.6 g/cm^3 solution of Sodium Polytungstate (SPT), $3Na_2WO_4 \cdot 9WO_3 \cdot H_2O$, for 24 hours to extract MP particles (figure 13). Density separation works by mixing the sample with a separation agent and, after mixing, lighter particles tend to float to the top layer of the mixture, while denser ones sink to the bottom (Frias et al., 2018) . After separation, the liquid, containing MPs, was filtered using the same type of filtration apparatus used for the water samples, with a dedicated filter for each sediment sample.

SPT was introduced in 1983 as a novel medium for density gradient separations (Plewinsky & Kamp, 1984). This non-toxic compound (Kazantzis, 1979) can be dissolved in water to create a liquid with an adjustable density, ranging from that of pure water at 1 g/cm^3 to a saturated solution with a density of 3.10 g/cm^3 (Skipp & Brownfield, 1993). Moreover, SPT offers additional benefits. It is non-corrosive, with a pH of 6 (Gregory & Johnston, 1987), and remains stable within a pH range of 2 to 14. Unlike flammable solvents used to dilute or wash other organic heavy liquids, SPT can be easily reclaimed and reused through a simple water wash. Since SPT is non-toxic, separations can be conducted without the need for a fume hood or personal protective equipment (Skipp & Brownfield, 1993).

In addition to its safety and environmental advantages, SPT proves to be highly effective across various applications, especially in sediment separation processes within geology and environmental studies. Its capability to create precise density gradients facilitates the efficient separation of heavy minerals and contaminants from sediment samples, which is essential for accurate analysis and reliable research results (Helbig & Pitt, 2018). The high density of SPT solutions, which can be adjusted to meet specific needs, allows for the separation of even the smallest and most challenging particles, making it a preferred alternative to traditional heavy liquids such as bromoform and methylene iodide (Skipp & Brownfield, 1993).

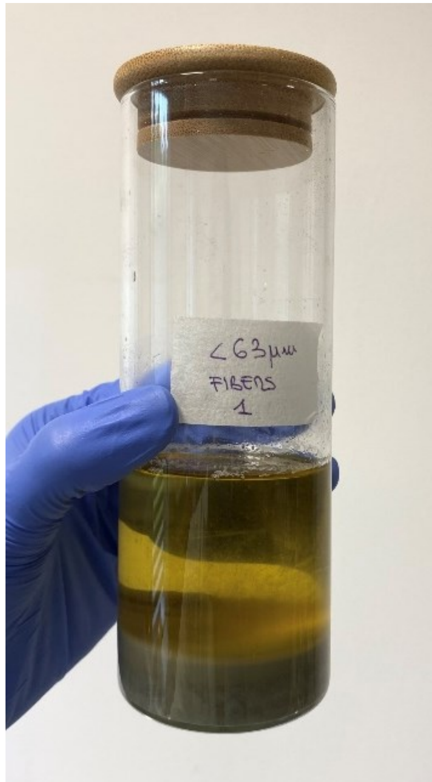

Figure 13: Density separation using SPT solution

MPs counting and calculation of sediment volumes

After filtration, the filters were photographed using a high-resolution camera (SONY ILCE-7RM3), ISO speed 100, with 300 dpi horizontal and vertical resolution. Subsequently, the MPs on the filters were counted manually using the Photoshop counting tool.

The 3D scans of the bed surface were utilized for a DoD analysis to quantify sediment movement and accumulation. Initially, photos of the bed were taken before and after the experiment of Run 3. These photos were then aligned using Agisoft Metashape software, creating a dense point cloud for each bed surface (figure 14, 15 respectively). Moreover, to accurately scale the dense cloud, six key markers were placed within the cloud, labeled as points 1 through 6. These markers were positioned based on known distances: 1-2: 0.07 m; 1-3: 0.14 m; 1-4: 0.508 m; 2-3: 0.07 m; 2-5: 0.503 m; 3-6: 0.497 m; 4-5: 0.07 m; 4-6: 0.14 m; 5-6: 0.07 m

The point clouds were saved in LAS format and imported into CloudCompare software. In CloudCompare, the point clouds were aligned and overlaid (figure 16), allowing for the calculation of volumetric differences between the two bed surfaces. After the point clouds were aligned and overlaid in CloudCompare, the DoD analysis was conducted to quantify sediment movement and accumulation. The DoD process involves subtracting the initial bed surface (before experiment) from the final bed surface (after experiment). This subtraction yields a difference map, where positive values indicate areas of sediment deposition, and negative values indicate areas of erosion (figure 17). The volumetric differences calculated from the DoD analysis provide precise insights into how sediment distribution and accumulation changed during the experiment. These differences were critical for understanding the impact of sediment transport and microplastic behavior in the flume.

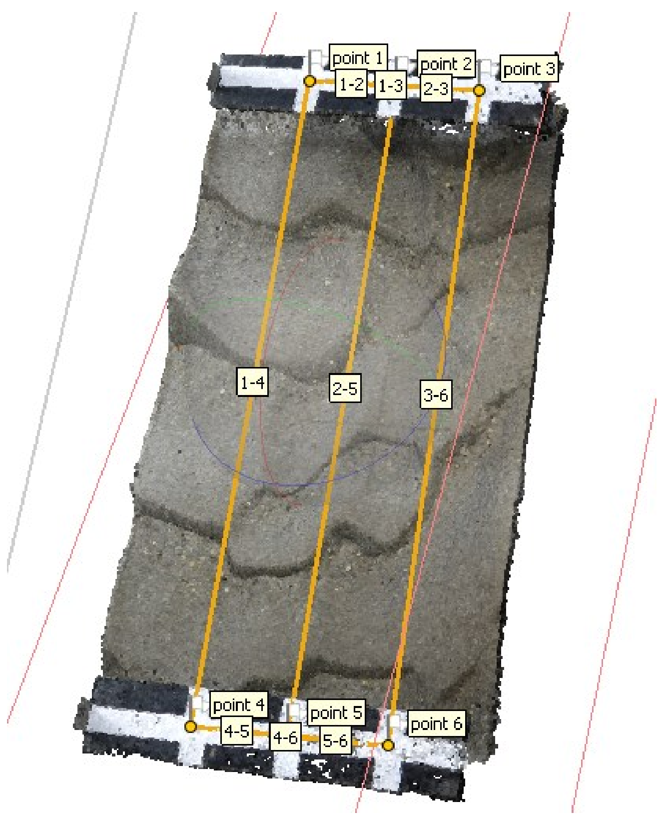

Figure 14: Dense cloud before the experiment

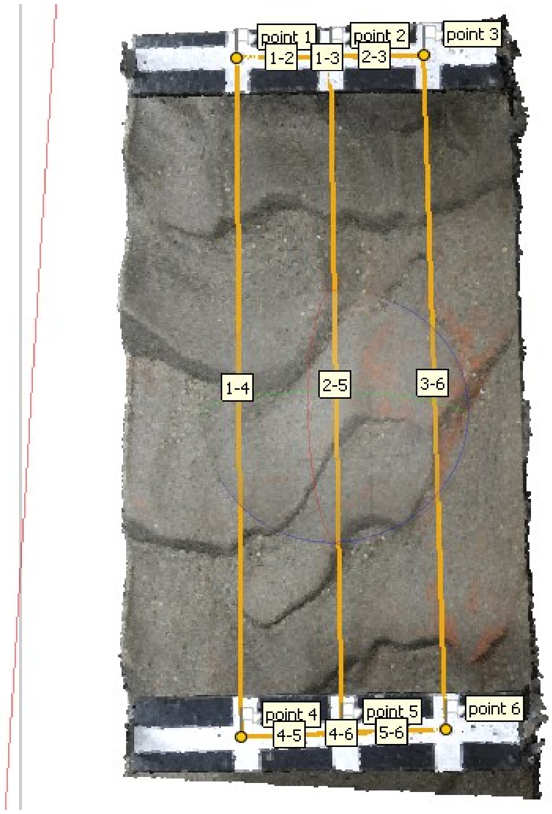

Figure 15: Dense cloud after the experiment

Figure 16: Alignment of the 2 dense cloud on CloudCompare software

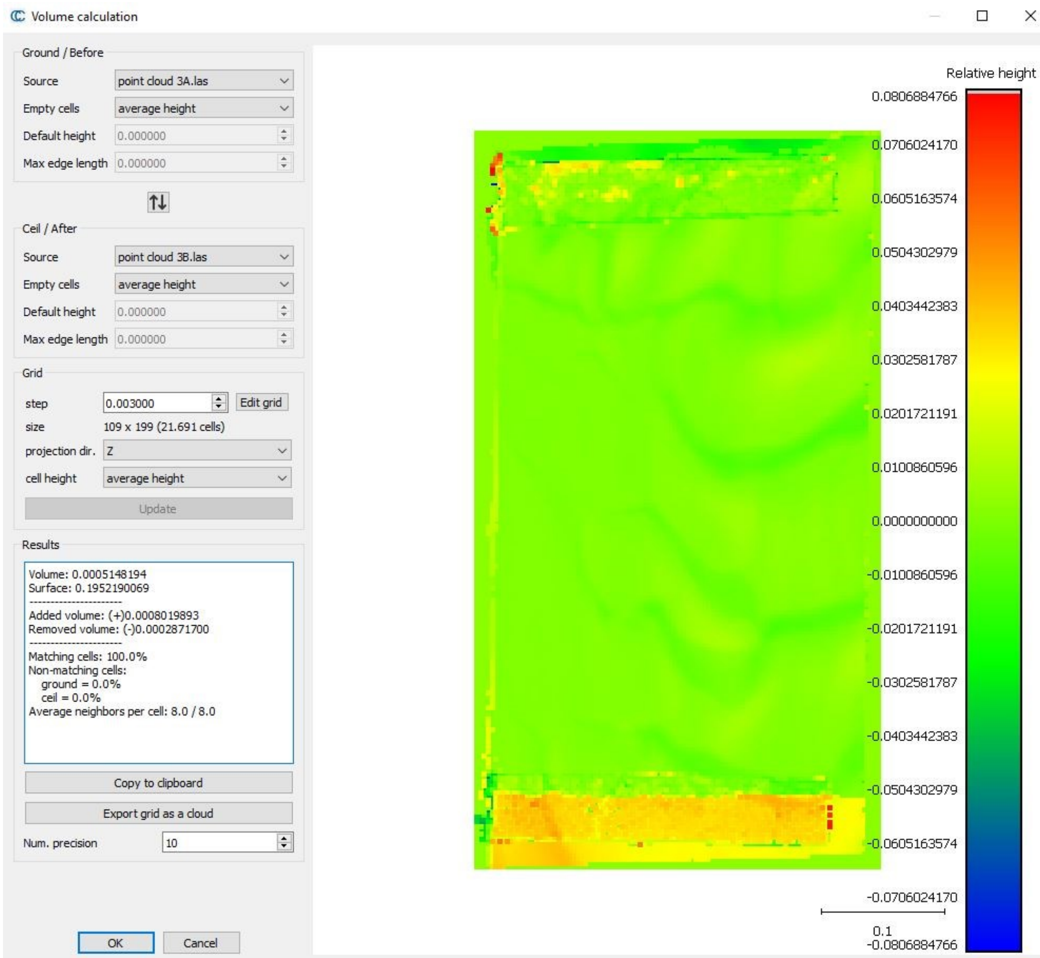

Figure 17: Volume calculation of the DoD on CloudCompare software

3. Results

This section presents the results from the two experiments conducted to study the behavior and distribution of MPs fibers in controlled conditions. Experiment 1 involved the introduction of MPs fibers into the channel, while Experiment 2 served as a run with MPs removal. Each experiment is conducted in two separate runs to ensure reproducibility. The results are categorized into MPs concentrations in water samples (upper part and lower part, closed to bedload surface, of the water column) and sediment samples (from five different ripple positions).

1. Results from Experiment 1
    a. Water samples

The water samples collected during Experiment 1 provide detailed information on the distribution of MPs fibers within the water column under controlled flow conditions. Table 2 summarizes the number of each fiber type across the two sampling methods.

	WATER SAMPLES											
	UPPER PART						**LOWER PART**					
	PA	PES	total	liters	**MPs/L (PA)**	**MPs/L (PES)**	PA	PES	total	liters	**MPs/L (PA)**	**MPs/L (PES)**
RUN 1	1048	1076	2124	1.6	655	672.5	968	1156	2124	1.6	605	722.5
RUN 2	1147	1420	2567	1.6	716.87	887.5	1214	1423	2637	1.6	758.75	889.37

Table 2: Number of MPs in water samples-Experiment 1

    b. Sediment samples

Sediment samples were taken only above the marker from 5 ripples within the channel during Experiment 1 to analyze how the introduced MPs fibers settled. The table 3 presents the results, showing how the fibers were distributed across different ripple positions within the sediment.

	SEDIMENT SAMPLES						
	PA	PES	total	Weight (g)	MPs/g (PA)	MPs/g (PES)	MPs/g (total)
RUN 1	17	40	57	20.00	0.85	2.00	2.85
RUN 1	13	23	36	20.00	0.65	1.15	1.80
RUN 1	13	56	69	20.00	0.65	2.8	3.45
RUN 1	13	50	63	20.00	0.65	2.50	3.15
RUN 1	11	35	46	20.00	0.55	1.75	2.30
RUN 2	2	10	12	25.19	0.08	0.40	0.48
RUN 2	7	13	20	23.21	0.31	0.57	0.88
RUN 2	9	19	28	20.28	0.44	0.93	1.37
RUN 2	4	14	18	20.00	0.20	0.7	0.90
RUN 2	7	22	29	20.00	0.35	1.10	1.45

Table 3: Number of MPs in sediment samples-Experiment 1

2. Results from Experiment 2
    a. Water samples

In experiment 2, water samples were analyzed to establish baseline MP concentrations in the absence of newly introduced MPs. Samples were collected from both the upper and lower parts of the flume to assess residual MP levels within the system, acknowledging that some MPs from Experiment 1 remained. This analysis was essential to differentiate between the residual MP levels and those observed after deliberate MPs introduction in Experiment 1. The results, detailed in Table 4, illustrate the background MP concentrations, providing a crucial reference point for understanding the system's response to MP presence under reduced concentration conditions.

	WATER SAMPLES											
	UPPER PART						LOWER PART					
	PA	PES	total	liters	**MPs/L (PA)**	**MPs/L (PES)**	PA	PES	total	liters	**MPs/L (PA)**	**MPs/L (PES)**
RUN 3	144	255	399	1.9	75.78	134.21	126	251	377	1.9	66.31	132.10
RUN 4	96	128	224	1.9	50.52	67.36	145	191	336	1.9	76.31	100.52

Table 4: Numbers of MPs in water samples-Experiment 2

b. Sediment samples

In Experiment 2, sediment samples were analyzed to determine the presence of residual MPs remaining from Experiment 1. Samples were taken from 5 ripples only above the marker to assess how the reduced concentration of MPs was distributed within the sediment. The findings, presented in Table 5, provide insight into the persistence and behavior of MPs in sediment under lower concentration conditions.

	SEDIMENT SAMPLES						
	PA	PES	total	Weight (g)	MPs/g (PA)	MPs/g (PES)	MPs/g (total)
RUN 3	0	3	3	18.00	0	0.16	0.16
RUN 3	0	4	4	21.50	0	0.18	0.18
RUN 3	0	2	2	21.30	0	0.09	0.09
RUN 3	1	8	9	24.10	0.04	0.33	0.37
RUN 3	1	5	6	25.00	0.04	0.2	0.24
RUN 4	1	0	0	20.00	0.05	0	0.05
RUN 4	0	3	3	20.20	0	0.14	0.14
RUN 4	2	4	6	16.00	0.12	0.25	0.37
RUN 4	0	7	7	17.30	0	0.40	0.40
RUN 4	0	7	7	16.10	0	0.43	0.43

Table 5: Numbers of MPs in sediment samples-Experiment 2

4. Discussion

The observed differences in the distribution of black PES fibers versus green PA fibers can be attributed to several factors, including differences in density, diameter, and variability in fiber size. Despite black PES fibers having a higher density (1.38 g/cm³) compared to green PA fibers (1.14 g/cm³), which would typically result in greater sedimentation, a higher concentration of black fibers was found in the water column. This indicates that factors beyond density, such as shape and size (see appendices 1), are at play, aligning with the findings of Waldschläger and Schüttrumpf (2019a), who highlighted that the relationship between density and settling velocity is complex and that particle shape and size significantly influence settling behavior.

In both "Experiment 1" and "Experiment 2", it was found that PES fibers maintained higher concentrations in the water column, particularly in the lower part near the bedload surface (Table 2). This finding suggests that other forces, such as drag and turbulence, may be suspending these fibers longer in the water. This is consistent with Boos et al. (2024), who demonstrated that microplastic particles are influenced by various hydrodynamic conditions in fluvial systems, causing larger particles to be retained in the water. This points to the significant role of physical forces like drag and mechanical straining in preventing full sedimentation of higher-density particles like PES fibers.

To further understand the relationship between microplastic particles in the water column and sedimentation, we conducted calculations to determine how much MPs suspension is required to trap a specific amount in the sediment. The total water volume passing through the flume was 2700 liters, coming from a discharge of 9 l/s during 5 minutes and considering the results of Run 3, the average concentration of MPs in the water samples was 102.1 MPs, the sediment accumulation was 0.8 liters given from the DoD from the added volume of 0.0008 m^3 (figure 17) with a sediment density of 2600 kg/m³, resulting in a total mass of 2.08 kg of sediment. From these measurements, we calculated that approximately 481.60 MPs would need to be present in the water to trap 1 microplastic in the sediment. However, in our experiments, we observed 777 MPs in the water and 24 MPs in the sediment, which corresponds to a ratio of roughly 32.4 MPs in the water for each MPs in the sediment. This deviation from our expected ratio can be attributed to several factors, including the specific sampling location, variability in particle sizes, and the efficiency of sediment trapping.

However, PES fibers were also dominant in the sediment samples across different ripple positions in “Experiment 1” (Table 3). This could be explained by particle infiltration dynamics, as shown in the work of Boos et al. (2021), which suggested that microplastic particles are retained in shallower sediment layers due to mechanical filtering. Moreover, particle size has been shown to play a critical role in infiltration, as larger fibers are more likely to be retained, even in sediment environments, as described in He et al. (2020).

In “Experiment 2”, the reduced concentration of MPs in both water and sediment samples (Table 4 and 5) demonstrates the persistence of MPs within the system, even after removal processes. This observation is in line with what is reported by Boos et al. (2024), who observed the infiltration and retention of microplastics within sediment layers, particularly during reduced flow or concentration conditions. Such findings further confirm the complexity of predicting microplastic distribution based solely on physical properties like density or size.

The complexity in fiber behavior underscores the inherent challenge in predicting MPs' environmental distribution based solely on density. In this study, despite adding equal masses (300 mg) of black PES and green PA fibers, a disproportionate distribution of fibers was observed between the water column and sediment layers. This indicates that mass alone does not determine the fate of MPs, but rather, their physical properties such as size (Waldschläger & Schüttrumpf, 2019a), shape (Hoellein et al., 2017), and even variability within these factors.

The disproportionate distribution observed in the experiments also suggests that MPs with similar mass can behave very differently due to variations in size and shape (Matjašič et al., 2023). For example, the larger diameter of PES fibers may have led to their increased suspension in the water column, while their irregular shapes likely contributed to a higher retention rate in the sediment. This reflects the studies of Kumar et al. (2021), who emphasized that hydrodynamic conditions, fiber shape, and particle size significantly impact the behavior of MPs in aquatic environments.

5. Conclusion and future work

The study highlights the complexity of microplastic behavior in a controlled flume experiment, emphasizing that factors such as fiber shape, size, and hydrodynamic conditions play a more significant role in their distribution than mass or density alone. While PES fibers, with a higher density, were expected to settle quickly in sediment, they remained suspended for longer periods due to their interaction with flow dynamics. This demonstrates that microplastics, even with similar physical properties, can behave very differently based on environmental factors. Furthermore, the pollution potential of microplastics is not solely determined by the number of fibers present, but also by their total length, surface area, and other physical characteristics. These aspects could significantly influence their environmental impact, including interactions with aquatic organisms and the potential for chemical adsorption. Therefore, future research should prioritize developing methodologies to quantify the total length and surface area of microplastic fibers as pollution metrics, providing a more comprehensive understanding of their behavior and risks.

References

Avio, C. G., Gorbi, S., Milan, M., Benedetti, M., Fattorini, D., d'Errico, G., Pauletto, M., Bargelloni, L., & Regoli, F. (2015). Pollutants bioavailability and toxicological risk from microplastics to marine mussels. *Environmental Pollution*, *198*, 211–222. https://doi.org/10.1016/j.envpol.2014.12.021

Ballent, A., Corcoran, P. L., Madden, O., Helm, P. A., & Longstaffe, F. J. (2016). Sources and sinks of microplastics in Canadian Lake Ontario nearshore, tributary and beach sediments. *Marine Pollution Bulletin*, *110*(1), 383–395. https://doi.org/10.1016/j.marpolbul.2016.06.037

Barnes, D. K. A., Galgani, F., Thompson, R. C., & Barlaz, M. (2009). Accumulation and fragmentation of plastic debris in global environments. *Philosophical Transactions of the Royal Society B: Biological Sciences*, *364*(1526), 1985–1998. https://doi.org/10.1098/rstb.2008.0205

Besseling, E., Quik, J. T. K., Sun, M., & Koelmans, A. A. (2017). Fate of nano- and microplastic in freshwater systems: A modeling study. *Environmental Pollution*, *220*, 540–548. https://doi.org/10.1016/j.envpol.2016.10.001

Boos, J., Dichgans, F., Fleckenstein, J. H., Gilfedder, B. S., & Frei, S. (2024). Assessing the Behavior of Microplastics in Fluvial Systems: Infiltration and Retention Dynamics in Streambed Sediments. *Water Resources Research*, *60*(2), e2023WR035532. https://doi.org/10.1029/2023WR035532

Boos, J., Gilfedder, B. S., & Frei, S. (2021). Tracking Microplastics Across the Streambed Interface: Using Laser-Induced-Fluorescence to Quantitatively Analyze Microplastic Transport in an Experimental Flume. *Water Resources Research*, *57*(12), e2021WR031064. https://doi.org/10.1029/2021WR031064

Browne, M. A., Crump, P., Niven, S. J., Teuten, E., Tonkin, A., Galloway, T., & Thompson, R. (2011). Accumulation of Microplastic on Shorelines Woldwide: Sources and Sinks. *Environmental Science & Technology*, *45*(21), 9175–9179. https://doi.org/10.1021/es201811s

Browne, M. A., Niven, S. J., Galloway, T. S., Rowland, S. J., & Thompson, R. C. (2013). Microplastic Moves Pollutants and Additives to Worms, Reducing Functions Linked to Health and Biodiversity. *Current Biology*, *23*(23), 2388–2392. https://doi.org/10.1016/j.cub.2013.10.012

Chua, E. M., Shimeta, J., Nugegoda, D., Morrison, P. D., & Clarke, B. O. (2014). Assimilation of Polybrominated Diphenyl Ethers from Microplastics by the Marine Amphipod, *Allorchestes Compressa*. *Environmental Science & Technology*, *48*(14), 8127–8134. https://doi.org/10.1021/es405717z

Chubarenko, I., Bagaev, A., Zobkov, M., & Esiukova, E. (2016). On some physical and dynamical properties of microplastic particles in marine environment. *Marine Pollution Bulletin*, *108*(1–2), 105–112. https://doi.org/10.1016/j.marpolbul.2016.04.048

Chubarenko, I., Esiukova, E., Bagaev, A., Isachenko, I., Demchenko, N., Zobkov, M., Efimova, I., Bagaeva, M., & Khatmullina, L. (2018). Behavior of Microplastics in Coastal Zones. In *Microplastic Contamination in Aquatic Environments* (pp. 175–223). Elsevier. https://doi.org/10.1016/B978-0-12-813747-5.00006-0

Corcoran, P. L., Belontz, S. L., Ryan, K., & Walzak, M. J. (2020). Factors Controlling the Distribution of Microplastic Particles in Benthic Sediment of the Thames River, Canada. *Environmental Science & Technology*, *54*(2), 818–825. https://doi.org/10.1021/acs.est.9b04896

Cowger, W., Gray, A. B., Guilinger, J. J., Fong, B., & Waldschläger, K. (2021). Concentration Depth Profiles of Microplastic Particles in River Flow and Implications for Surface Sampling. *Environmental Science & Technology*, *55*(9), 6032–6041. https://doi.org/10.1021/acs.est.1c01768

Coyle, R., Hardiman, G., & Driscoll, K. O. (2020). Microplastics in the marine environment: A review of their sources, distribution processes, uptake and exchange in ecosystems. *Case Studies in Chemical and Environmental Engineering*, *2*, 100010. https://doi.org/10.1016/j.cscee.2020.100010

De Falco, F., Gullo, M. P., Gentile, G., Di Pace, E., Cocca, M., Gelabert, L., Brouta-Agnésa, M., Rovira, A., Escudero, R., Villalba, R., Mossotti, R., Montarsolo, A., Gavignano, S., Tonin, C., & Avella, M. (2018). Evaluation of microplastic release caused by textile washing processes of synthetic fabrics. *Environmental Pollution*, *236*, 916–925. https://doi.org/10.1016/j.envpol.2017.10.057

Enders, K., Käppler, A., Biniasch, O., Feldens, P., Stollberg, N., Lange, X., Fischer, D., Eichhorn, K.-J., Pollehne, F., Oberbeckmann, S., & Labrenz, M. (2019). Tracing microplastics in aquatic environments based on sediment analogies. *Scientific Reports*, *9*(1), 15207. https://doi.org/10.1038/s41598-019-50508-2

Francalanci, S., Paris, E., & Solari, L. (2021). On the prediction of settling velocity for plastic particles of different shapes. *Environmental Pollution*, *290*, 118068. https://doi.org/10.1016/j.envpol.2021.118068

Frias, J. P. G. L., Pagter, E., Nash, R., O'Connor, I., Carretero, O., Filgueiras, A., Viñas, L., J. Gago, Antunes, J. C., Bessa, F., Sobral, P., Goruppi, A., Tirelli, V., Pedrotti, M. L., Suaria, G., Aliani, S., Lopes, C., Raimundo, J., Caetano, M., … Gerdts, G. (2018). *Standardised protocol for monitoring microplastics in sediments*. https://doi.org/10.13140/RG.2.2.36256.89601/1

Ghinassi, M., Michielotto, A., Uguagliati, F., & Zattin, M. (2023). Mechanisms of microplastics trapping in river sediments: Insights from the Arno river (Tuscany, Italy). *Science of The Total Environment*, *866*, 161273. https://doi.org/10.1016/j.scitotenv.2022.161273

Gregory, M. R., & Johnston, K. A. (1987). *A Nontoxic Substitute for Hazardous Heavy Liquids—Aqueous Sodium Polytungstate (3Na2WO4.9WO3.H2O) Solution*. https://doi.org/10.1080/00288306.1987.10552626

He, B., Wijesiri, B., Ayoko, G. A., Egodawatta, P., Rintoul, L., & Goonetilleke, A. (2020). Influential factors on microplastics occurrence in river sediments. *Science of The Total Environment*, *738*, 139901. https://doi.org/10.1016/j.scitotenv.2020.139901

Helbig, P., & Pitt, C. D. (2018). Sodium polytungstate as gravity separating fluid for polymeric blasting media evaluation. *Analytical Methods*, *10*(25), 3039–3042. https://doi.org/10.1039/C8AY00946E

Hernandez, E., Nowack, B., & Mitrano, D. M. (2017). Polyester Textiles as a Source of Microplastics from Households: A Mechanistic Study to Understand Microfiber Release During Washing. *Environmental Science & Technology*, *51*(12), 7036–7046. https://doi.org/10.1021/acs.est.7b01750

Hidalgo-Ruz, V., Gutow, L., Thompson, R. C., & Thiel, M. (2012). Microplastics in the Marine Environment: A Review of the Methods Used for Identification and Quantification. *Environmental Science & Technology*, *46*(6), 3060–3075. https://doi.org/10.1021/es2031505

Hoellein, T. J., McCormick, A. R., Hittie, J., London, M. G., Scott, J. W., & Kelly, J. J. (2017). Longitudinal patterns of microplastic concentration and bacterial assemblages in surface and benthic habitats of an urban river. *Freshwater Science*, *36*(3), 491–507. https://doi.org/10.1086/693012

Horton, A. A., Svendsen, C., Williams, R. J., Spurgeon, D. J., & Lahive, E. (2017). Large microplastic particles in sediments of tributaries of the River Thames, UK – Abundance, sources and methods for effective quantification. *Marine Pollution Bulletin*, *114*(1), 218–226. https://doi.org/10.1016/j.marpolbul.2016.09.004

Kaiser, D., Kowalski, N., & Waniek, J. J. (2017). Effects of biofouling on the sinking behavior of microplastics. *Environmental Research Letters*, *12*(12), 124003. https://doi.org/10.1088/1748-9326/aa8e8b

Kazantzis, G. (1979). *Tungsten*. 639–645.

Kooi, M., Nes, E. H. V., Scheffer, M., & Koelmans, A. A. (2017). Ups and Downs in the Ocean: Effects of Biofouling on Vertical Transport of Microplastics. *Environmental Science & Technology*, *51*(14), 7963–7971. https://doi.org/10.1021/acs.est.6b04702

Kumar, R., Sharma, P., Verma, A., Jha, P. K., Singh, P., Gupta, P. K., Chandra, R., & Prasad, P. V. V. (2021). Effect of Physical Characteristics and Hydrodynamic Conditions on Transport and Deposition of Microplastics in Riverine Ecosystem. *Water*, *13*(19), 2710. https://doi.org/10.3390/w13192710

Lebreton, L. C. M., Van Der Zwet, J., Damsteeg, J.-W., Slat, B., Andrady, A., & Reisser, J. (2017). River plastic emissions to the world's oceans. *Nature Communications*, *8*(1), 15611. https://doi.org/10.1038/ncomms15611

Liro, M., Emmerik, T. V., Wyżga, B., Liro, J., & Mikuś, P. (2020). Macroplastic Storage and Remobilization in Rivers. *Water*, *12*(7), 2055. https://doi.org/10.3390/w12072055

Liu, L., Xu, M., Ye, Y., & Zhang, B. (2022). On the degradation of (micro)plastics: Degradation methods, influencing factors, environmental impacts. *Science of The Total Environment*, *806*, 151312. https://doi.org/10.1016/j.scitotenv.2021.151312

Lu, L., Tang, Q., Li, H., & Li, Z. (2022). Damming river shapes distinct patterns and processes of planktonic bacterial and microeukaryotic communities. *Environmental Microbiology*, *24*(4), 1760–1774. https://doi.org/10.1111/1462-2920.15872

Lusher, A. L., Burke, A., O'Connor, I., & Officer, R. (2014). Microplastic pollution in the Northeast Atlantic Ocean: Validated and opportunistic sampling. *Marine Pollution Bulletin*, *88*(1–2), 325–333. https://doi.org/10.1016/j.marpolbul.2014.08.023

Matjašič, T., Mori, N., Hostnik, I., Bajt, O., & Kovač Viršek, M. (2023). Microplastic pollution in small rivers along rural–urban gradients: Variations across catchments and between water column and sediments. *Science of The Total Environment*, *858*, 160043. https://doi.org/10.1016/j.scitotenv.2022.160043

Napper, I. E., & Thompson, R. C. (2016). Release of synthetic microplastic plastic fibres from domestic washing machines: Effects of fabric type and washing conditions. *Marine Pollution Bulletin*, *112*(1–2), 39–45. https://doi.org/10.1016/j.marpolbul.2016.09.025

Nel, H. A., Hean, J. W., Noundou, X. S., & Froneman, P. W. (2017). Do microplastic loads reflect the population demographics along the southern African coastline? *Marine Pollution Bulletin*, *115*(1–2), 115–119. https://doi.org/10.1016/j.marpolbul.2016.11.056

PlascticEurope. (2021). An analysis of European plastics production, demand and waste data. *Plastics-the Facts 2021*.

Plewinsky, B., & Kamp, R. (1984). Sodium metatungstate, a new medium for binary and ternary density gradient centrifugation: *Makromolekulare Chemie*, *185*.

Rillig, M. C. (2012). Microplastic in Terrestrial Ecosystems and the Soil? *Environmental Science & Technology*, *46*(12), 6453–6454. https://doi.org/10.1021/es302011r

Sekudewicz, I., Dąbrowska, A. M., & Syczewski, M. D. (2021). Microplastic pollution in surface water and sediments in the urban section of the Vistula River (Poland). *Science of The Total Environment*, *762*, 143111. https://doi.org/10.1016/j.scitotenv.2020.143111

Skipp, G. L., & Brownfield, I. (1993). *Open-File Report* (Open-File Report) [Open-File Report].

Sun, J., Lin, Z., Ning, D., Wang, H., Zhang, Z., He, Z., & Zhou, J. (2022). Functional microbial community structures and chemical properties indicated mechanisms and potential risks of urban river eco-remediation. *Science of The Total Environment*, *803*, 149868. https://doi.org/10.1016/j.scitotenv.2021.149868

Tamilmani, A., & Venkatesan, G. (2021). Assessment of trace metals and its pollution load indicators in water and sediments between Upper and Grand Anicuts in the Cauvery. *International Journal of Environmental Science and Technology*, *18*(12), 3807–3818. https://doi.org/10.1007/s13762-020-03034-y

Toraskar, A. D., Manohar, C. S., Fernandes, C. L., Ray, D., Gomes, A. D., & Antony, A. (2022). Seasonal variations in the water quality and antibiotic resistance of microbial pollution indicators in the Mandovi and Zuari estuaries, Goa, India. *Environmental Monitoring and Assessment*, *194*(2), 71. https://doi.org/10.1007/s10661-021-09679-7

Vimalkumar, K., Arun, E., Krishna-Kumar, S., Poopal, R. K., Nikhil, N. P., Subramanian, A., & Babu-Rajendran, R. (2018). Occurrence of triclocarban and benzotriazole ultraviolet stabilizers in water, sediment, and fish from Indian rivers. *Science of The Total Environment*, *625*, 1351–1360. https://doi.org/10.1016/j.scitotenv.2018.01.042

Waldschläger, K., Brückner, M. Z. M., Carney Almroth, B., Hackney, C. R., Adyel, T. M., Alimi, O. S., Belontz, S. L., Cowger, W., Doyle, D., Gray, A., Kane, I., Kooi, M., Kramer, M., Lechthaler, S., Michie, L., Nordam, T., Pohl, F., Russell, C., Thit, A., … Wu, N. (2022). Learning from natural sediments to tackle microplastics challenges: A multidisciplinary perspective. *Earth-Science Reviews*, *228*, 104021. https://doi.org/10.1016/j.earscirev.2022.104021

Waldschläger, K., Lechthaler, S., Stauch, G., & Schüttrumpf, H. (2020). The way of microplastic through the environment – Application of the source-pathway-receptor model (review). *Science of The Total Environment*, *713*, 136584. https://doi.org/10.1016/j.scitotenv.2020.136584

Waldschläger, K., & Schüttrumpf, H. (2019a). Effects of Particle Properties on the Settling and Rise Velocities of Microplastics in Freshwater under Laboratory Conditions. *Environmental Science & Technology*, *53*(4), 1958–1966. https://doi.org/10.1021/acs.est.8b06794

Waldschläger, K., & Schüttrumpf, H. (2019b). Erosion Behavior of Different Microplastic Particles in Comparison to Natural Sediments. *Environmental Science & Technology*, *53*(22), 13219–13227. https://doi.org/10.1021/acs.est.9b05394

Welden, N. A., & Lusher, A. L. (2017). Impacts of changing ocean circulation on the distribution of marine microplastic litter. *Integrated Environmental Assessment and Management*, *13*(3), 483–487. https://doi.org/10.1002/ieam.1911

Xia, W., Rao, Q., Deng, X., Chen, J., & Xie, P. (2020). Rainfall is a significant environmental factor of microplastic pollution in inland waters. *Science of The Total Environment*, *732*, 139065. https://doi.org/10.1016/j.scitotenv.2020.139065

Yang, L., Zhang, Y., Kang, S., Wang, Z., & Wu, C. (2021). Microplastics in freshwater sediment: A review on methods, occurrence, and sources. *Science of The Total Environment*, *754*, 141948. https://doi.org/10.1016/j.scitotenv.2020.141948

Zhang, D., Cui, Y., Zhou, H., Jin, C., Yu, X., Xu, Y., Li, Y., & Zhang, C. (2020). Microplastic pollution in water, sediment, and fish from artificial reefs around the Ma'an Archipelago, Shengsi, China. *Science of The Total Environment*, *703*, 134768. https://doi.org/10.1016/j.scitotenv.2019.134768

Appendices

App.1: Filter from the water sample showing the distribution of different sizes for the PES fibers

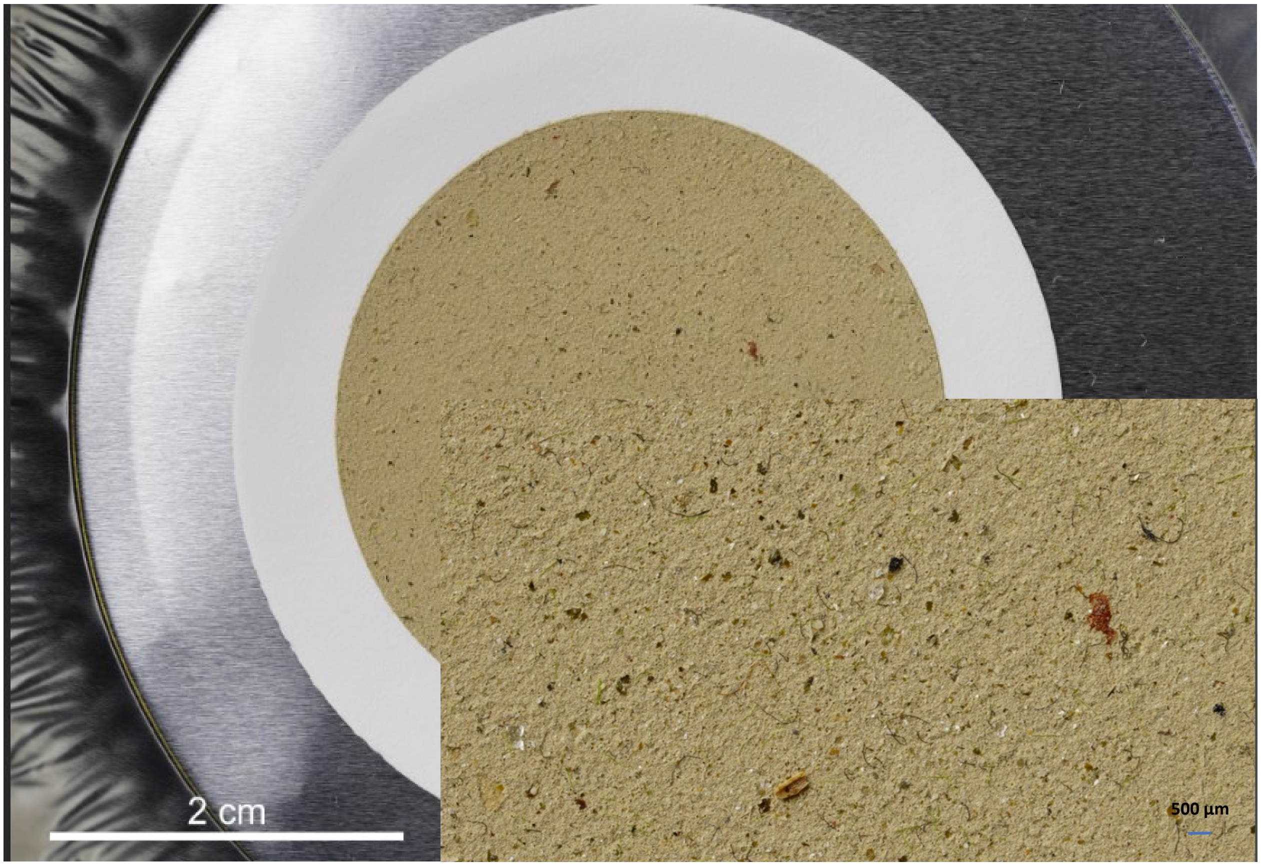

App.2: Filter from the water sample showing the distribution of PA and PES fibers

Acknowledgment

I would like to express my deepest gratitude to my supervisors, Prof. Massimiliano Zattin, Prof. Massimiliano Ghinassi, Dr. Francesca Uguagliati for their unwavering support, guidance, and insight throughout the course of this project. Their mentorship was invaluable and shaped the direction of my research in meaningful ways.

Special thanks go to the technical staff, Prof. Silvia Cattò, M. Stefano Castelli for their expertise and assistance that made my journey much smoother.

I am also thankful to the members of my thesis committee, for taking the time to evaluate this thesis.

Likewise, I want to express my heartfelt gratitude to family and my friends for their constant encouragement and patience. Their support and prayers kept me motivated, even in the most challenging times.

And above all for His unconditional love, my Lord, thank you.